Metamaterial coatings for broadband asymmetric mirrors

A. Chen,[1] K. Hasegawa,[1] V. A. Podolskiy,[2] and M. Deutsch[1,*]

[1]*Department of Physics, University of Oregon, Eugene, Oregon 97403, USA*
[2]*Department of Physics, Oregon State University, Corvallis, Oregon 97331, USA*
**Corresponding author: miriamd@uoregon.edu*

Received February 21, 2007; revised April 20, 2007; accepted April 23, 2007;
posted April 25, 2007 (Doc. ID 80299); published June 18, 2007

We report the design and fabrication of nanostructured metal–dielectric mirrors with high reflectance asymmetries in the visible spectral range. Applying dispersion engineering principles to model a broadband and large reflectance asymmetry, we obtain a dielectric function for this metamaterial, closely resembling the effective permittivity of disordered metal–dielectric nanocomposites. Coatings realized by using disordered nanocrystalline silver films on glass substrates confirm the theoretical predictions, exhibiting symmetric transmittance, accompanied by large broadband reflectance asymmetries.

OCIS codes: 310.6860, 230.4040, 260.2030.

Optical metamaterials—artificial composites with an engineered electromagnetic response—hold the potential for greatly affecting modern photonics, with applications to novel guiding, imaging, and dispersive components [1–4]. The two main classes of metamaterials comprise disordered metallodielectrics [5,6] and ordered materials such as photonic crystals [7]. In this Letter we demonstrate an application of disordered materials that harnesses their dispersive properties. In particular, we implement disordered metal–dielectric films to achieve highly asymmetric broadband optical reflectors.

An asymmetric mirror is an optical device exhibiting asymmetry in reflectance of light incident from either side, while its transmittance is symmetric [8]. The energy-balance relations are $T+R_{1,2}+A_{1,2}=1$, where T, R, and A denote transmittance, reflectance, and losses (in the form of absorption as well as scattering), respectively, and the subscripts 1 and 2 specify the direction of light incidence. Asymmetric mirrors have recently found use in Fabry–Perot interferometers [9]. To obtain such a mirror, two conditions must hold: (i) the structure must lack inversion symmetry, and (ii) the mirror should impart a nonunitary energy transformation. The latter may be achieved through out-of-beam scattering or by ensuring that the dielectric function of at least one of the films is complex, i.e., exhibiting absorptive losses or gain. One of the simplest structures for an asymmetric mirror is a thin metal film on a dielectric slab, embedded in vacuum.

Asymmetric mirrors have been realized by using smooth metal films on planar substrates [10,11], or gratings [12]. The reflectance asymmetries and bandwidths of such mirrors are typically constrained to a narrow range, due to the limited choice of materials. We show that these characteristics are dramatically enhanced in metamaterials.

By solving Maxwell's equations for an electromagnetic field of frequency ω impinging on a film of thickness d and permittivity ϵ_f, deposited on a semi-infinite substrate embedded in vacuum, the reflectance asymmetry is obtained as

$$\Delta R \equiv R_1 - R_2 = \frac{|AB+C|^2 - |AC+B|^2}{|1+ABC|^2}. \tag{1}$$

Here $A \equiv e^{2ik_f d}$, with $k_f = \sqrt{\epsilon_f}\omega/c$. We limit our model to absorptive films, i.e., $\epsilon_f \equiv \epsilon_f' + i|\epsilon_f''|$. The amplitude reflection coefficients $B \equiv r_{12}$, $C \equiv r_{23}$ denote reflections from the vacuum–metal and metal–dielectric interfaces, respectively. Rewriting the numerator above as $(|A|^2-1)(|B|^2-|C|^2)+2\ \mathrm{Re}[A(BC^*-B^*C)]$, we see that $\Delta R=0$ in systems with inversion symmetry, where $B=-C$, or for lossless materials, where either $|A|=1$ and B and C are real (lossless dielectrics) or $|B|=|C|=1$ and $A(BC^*-B^*C)$ is pure imaginary (lossless metals.)

It is important to understand the dependence of ΔR on the parameters of the metal, and in particular on optical losses. This is instrumental in designing asymmetric mirrors with controllable spectral response. Since ϵ_f of the metal is a function of frequency, a closed-form expression for ΔR is not always available. In Fig. 1(a) we plot ΔR of a silver film on a 1 mm thick glass slab embedded in vacuum [13]. Without loss of generality we limit our analysis to normal incidence. Close examination of ΔR reveals frequency dependence, due to material dispersion as well as finite film thickness effects, while its value in the minimum dispersion range is only ~2%. This behavior is typical of most metals that are reflective in

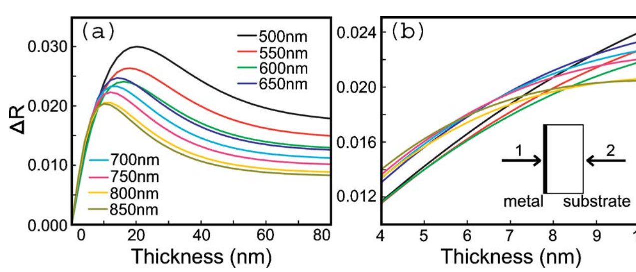

Fig. 1. (Color online) (a) Dependence of ΔR on film thickness. (b) Magnified view of the near crossover in (a). Inset, schematic of mirror; numbers denote the direction of incidence.

0146-9592/07/131770-3/$15.00

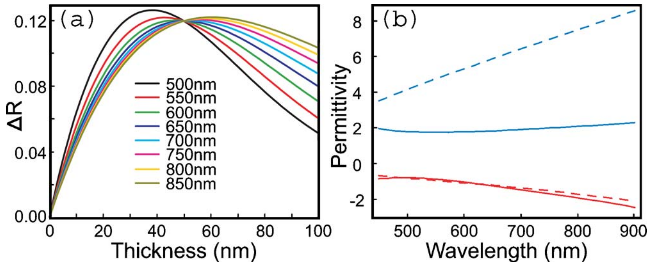

Fig. 2. (Color online) (a) Asymmetry of dispersion-engineered film on glass substrate, showing exact crossover at $d=50$ nm. (b) Solid curves, real (red, lower) and imaginary (blue, higher) components of ϵ_f obtained from inverting ΔR in (a). Dashed lines, best fits of ϵ_f' and ϵ_f'' obtained using Bruggemann EMT.

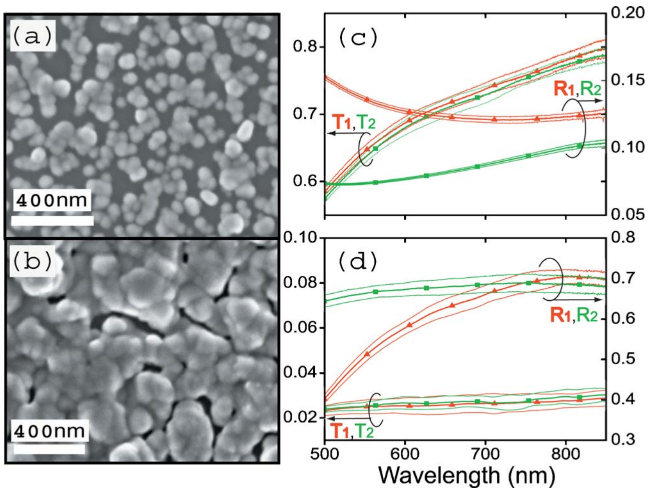

Fig. 3. (Color online) Left: SEM images of films with different metal ratios, p=: (a) 0.52, (b) 0.93. Right: (c), (d) Measured $R_{1,2}$ and $T_{1,2}$ of films at left. Heavy curves, measured values; thin curves denote the range of error.

the visible and near-infrared (NIR). We stress that the existence of $\Delta R \neq 0$ does not rely on a resonance condition in the metal or substrate and is possible for any film and substrate thicknesses as long as the conditions stated previously are fulfilled. Certain applications (e.g., in solar cells) may benefit from larger $|\Delta R|$, with simultaneous minimization of its dispersion. This requires careful design of the film's structure and composition, yielding a dispersion-engineered material.

We start by imposing two constraints: (i) ΔR should be large (~10%) and (ii) ΔR should possess a broadband characteristic, i.e., $\partial(\Delta R)/\partial\lambda=0$ at a given film thickness. As an example, we select the functional form of ΔR to resemble Fig. 1(a). As substrate we choose nondispersive glass ($\epsilon \simeq 2.3$), which is similar to many transparent dielectrics used in visible and NIR applications. The broadband condition implies the existence of a design parameter—the film thickness, d—at a particular value of which ΔR is constant over a wide spectral range. This (exact) crossover point in ΔR is chosen at $d=50$ nm. Such crossover may be generated for any film and substrate thickness. Figure 2(a) shows ΔR plotted against d. The function $\epsilon_f(\lambda)$ is extracted from ΔR by simple inversion. For a given form of ΔR, there exist a wide range of values of d $(0<d\simeq 50\text{ nm})$ and ΔR (up to ~15%) for which the resulting $\epsilon_f(\lambda)$ exhibits the general form expected for a material satisfying the causality relations.

The resulting dielectric response is shown in Fig. 2(b). We see that $\epsilon_f'<0$ over the entire visible and NIR range, implying a metallic response. We note that ϵ_f'' is significantly greater than permittivities of metals compatible with optical applications (e.g., gold and silver) while $|\epsilon_f'|$ is considerably smaller.

While the desired ϵ_f differs from that of known materials, a dielectric function similar to Fig. 2(b) may be achieved in metamaterials, often described by effective medium theory (EMT). According to EMT, materials with spatial inhomogeneities much smaller in size than the wavelength may be regarded as homogeneous on average. To demonstrate our design we apply Bruggemann EMT [14] to model a film with metal filling fraction p. The effective dielectric function ϵ_{eff} is given by

$$p\frac{\epsilon_m-\epsilon_{\text{eff}}}{g\epsilon_m+(1-g)\epsilon_{\text{eff}}}+(1-p)\frac{\epsilon_d-\epsilon_{\text{eff}}}{g\epsilon_d+(1-g)\epsilon_{\text{eff}}}=0, \quad (2)$$

where ϵ_m and ϵ_d are known dielectric functions of the metal and the dielectric, respectively, and $g=0.68$ is a constant describing the microscopic morphology of the film's constituents and is also known as the depolarization factor [15]. Note that we have introduced a second design parameter in the form of p [16].

The dashed lines in Fig. 2(b) show the results of EMT modeling of a silver nanocomposite embedded in vacuum. We find that a value of $p=0.71$ yields excellent agreement with the desired ϵ_f'. The discrepancy in the modeling ϵ_f'' is due to the microscopic loss mechanisms specific to the Bruggemann model, which cannot exactly reproduce the desired response.

Silver films of varying filling fractions were deposited on 1 mm thick glass slides by using a modified Tollen's reaction [17]. Scanning electron micrographs (SEMs) in Fig. 3 show typical morphologies of these films. Surface coverage was controlled by monitoring the deposition time, with reactions lasting from 1 to 6 h. The metal filling fractions ranged from $p\approx 0.1$ to $p\approx 0.9$ and were determined from high-resolution SEM images [18]. Respective film thicknesses as determined from atomic force microscopy ranged from $d\approx 10$ nm to $d\approx 50$ nm. Ensuing deposition samples were stored under nitrogen.

Optical reflectance and transmittance spectra were collected by using a microscope whose output was imaged on the entrance slit of an $F=320$ mm spectrometer with a resolution of 0.5 nm. Reflected and transmitted signals from a tungsten–halogen white-light source impinging normally on each side of the sample were collected with a 10× objective (0.25 N.A.) [19] and imaged onto a cooled detector. Reflected signals were carefully normalized by using a high-reflectance mirror (Newport Broadband SuperMirror, $R\geq 99.9\%$.) To eliminate spurious effects from local inhomogeneities, data from ~1000 μm across the

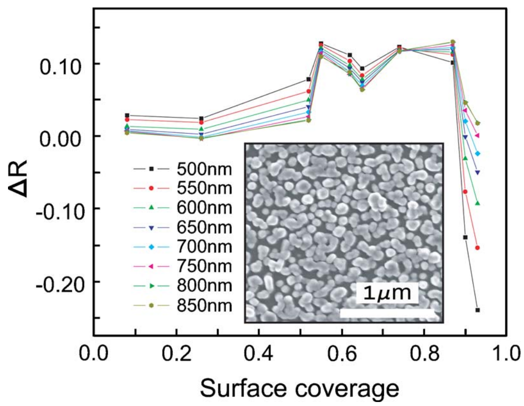

Fig. 4. (Color online) Reflectance asymmetry measured as function of p. Inset, SEM micrograph of $p=0.74$ film.

film were averaged. Various degrees of reflectance asymmetry were observed for films with different filling fractions. Nevertheless, the transmittance always remained symmetric, even for rough and dense films, as shown in Figs. 3(c) and 3(d). The latter indicates that the transmission symmetry is not broken by disorder-mediated (i.e., diffuse) scattering from the rough interfaces.

We now address the effect of the metal filling fraction on the reflectance asymmetry. In Fig. 4 we plot ΔR of 10 different samples. Both the magnitude and sign of ΔR depend strongly on surface coverage. Comparing this plot with the predicted model in Fig. 2(a) yields good agreement for the general shape of ΔR as well as for its target value of $\Delta R \sim 10\%$. We note that instead of plotting $\Delta R(d)$, we plot it against p, as the latter can be measured with much higher accuracy than the thickness of these rough films. Nevertheless, it is still possible to replace p with d and directly compare the data with theory. The most noticeable feature is the theoretically predicted crossover near $p=0.74$, where the dispersion in ΔR is minimal.

Comparing Fig. 4 to Fig. 2(a), we find discrepancies near $p=0.6$. This is not surprising, since EMTs such as the Bruggemann approach, while resembling the response of metamaterials, are often inadequate for describing losses. In particular, scattering boundary conditions are usually poorly known for discontinuous films, where surface scattering and enhanced absorption dominate. Indeed, we have computed ϵ_f of our films by using measured values of p and Eq. (2), but were not able to reproduce the asymmetry for most samples. This suggests that both ϵ_f' and ϵ_f'' are important in determining ΔR. Hence, to achieve a desired ΔR *ab initio*, we should not only optimize ϵ_f' but also account better for losses.

Our approach may be used to design metamaterial-based devices. Loss-compensated asymmetric mirrors may be realized by incorporating a gain medium into the embedding matrix [20]. Alternately, electroactive or semiconducting matrices may make it possible to implement these mirrors in photonic devices and solar cells.

In summary, we realized strongly asymmetric mirrors by using disordered silver films on glass substrates. Basic dispersion engineering principles were applied to model a broadband reflectance asymmetry, which was then inverted to yield the effective permittivity. An effective-medium approach was implemented to approximate the required optical response function in a metal–dielectric metamaterial, closely mimicking that of disordered silver–dielectric composites. The dependence of ΔR on the metal filling fraction was measured, demonstrating the predicted broadband characteristic.

This work was supported by National Science Foundation grant DMR-02-39273.

References

1. M. Bloemer, G. D Aguanno, M. Scalora, and N. Mattlucci, Appl. Phys. Lett. **87**, 261921 (2005).
2. J. B. Pendry, Phys. Rev. Lett. **85**, 3966 (2000).
3. Z. Jacob, L. Alexeyev, and E. Narimanov, Opt. Express **14**, 8247 (2006).
4. S. I. Bozhevolnyi, V. S. Volkov, and K. Leosson, Phys. Rev. Lett. **89**, 186801 (2002).
5. Th. Ung, L. M. Liz-Marzan, and P. Mulvaney, J. Phys. Chem. B **105**, 3441 (2001).
6. Y. Ding, Y. J. Kim, and J. Erlebacher, Adv. Mater. **16**, 1897 (2004).
7. T. A. Kelf, Y. Sugawara, J. J. Baumberg, M. Abdelsalam, and P. N. Bartlett, Phys. Rev. Lett. **95**, 116802 (2005).
8. P. G. Kard, Opt. Spectrosc. **10**, 193 (1963).
9. Yu. V. Troitskiǐ, Opt. Spectrosc. **98**, 125 (2005).
10. N. D. Goldina, Optics Spectrosc. **47**, 428 (1979).
11. Yu. V. Troitskiǐ, J. Opt. Soc. Am. A **15**, 261 (1998).
12. B. Bai, L. Li, and L. Zeng, Opt. Lett. **30**, 2360 (2005).
13. Spectral averaging over 0.5 nm intervals was employed.
14. D. Bruggeman, Ann. Phys. (Leipzig) **24**, 6736 (1935).
15. R. W. Cohen, G. D. Cody, M. D. Coutts, and B. Abeles, Phys. Rev. B **8**, 3689 (1973).
16. While p is the only EMT parameter for disordered films, the response of other classes of metamaterials may also depend on additional parameters such as shape (i.e., g), size, order, and permittivities of the constituents. The parameters describing these characteristics will impose additional constraints on the design process.
17. M. S. M. Emmons, J. Bouwman, A. Chen, and M. Deutsch, J. Colloid Interface Sci. **306**, 41 (2007).
18. C. A. Rohde, K. Haegawa, and M. Deutsch, Phys. Rev. Lett. **96**, 045503 (2006).
19. Calculations show that ΔR depends weakly on the angle near normal incidence; thus the experimental conditions are well approximated by the plane-wave modeling applied here, and no further angular averaging was necessary.
20. M. A. Noginov, G. Zhu, M. Bahoura, J. Adegoke, C. E. Small, B. A. Ritzo, V. P. Drachev, and V. M. Shalaev, Opt. Lett. **31**, 3022 (2006).